Journal of Orthopaedic Translation 28 (2021) 1–9

Contents lists available at ScienceDirect

Journal of Orthopaedic Translation

journal homepage: www.journals.elsevier.com/journal-of-orthopaedic-translation

Original article

The effect of topical administration of simvastatin on entochondrostosis and intramembranous ossification: An animal experiment

Lei Dang [a], Jinglin Zhu [b], Chunli Song [a,*]

[a] Department of Orthopedics, Peking University 3rd Hospital, Beijing Key Laboratory of Spinal Disease Research, Beijing, PR China
[b] Department of Orthopedics, Beijing Shijitan Hospital, Beijing, PR China

ARTICLE INFO

Keywords:
Simvastatin
Bone regeneration
Bone substitute
Entochondrostosis
Intramembranous ossification

ABSTRACT

Background: Simvastatin, a drug for lowering serum cholesterol, has been shown to enhance bone regeneration, but few studies have qualitatively and quantitatively tested its effect when used topically in different animal models. This study aims to investigate topical administration of simvastatin as a bone regeneration inducer by testing its effect on bone formation in both long tubular bone and flat bone defect, and the mechanism involved.
Methods: Two animal models were used for testing the effect of simvastatin on entochondrostosis and intramembranous ossification respectively. Simvastatin of different dosages combined with poly lactic acid were implanted in extreme radial defects of 12 adult male New Zealand rabbits. Bone formation was monitored using x-ray and CT-scan and measured using x-ray scales, pixel values and spiral CT-scan for 16 weeks before being subject to histological and immunohistochemistry examination. The result was compared with that of autograft and blank control groups. Simvastatin with thrombin and fibrin sealant were implanted in calvarial defects of three Rhesus monkeys and monitored for 18 weeks. Bone formation was compared between the simvastatin and the blank control group using spiral CT-scan and histological examination.
Results: Both visual and quantitative measurements by x-ray and spiral CT-scan indicated significant bone formation in radial defects in all simvastatin groups and the autograft group whereas no bone formation was found in control groups. There was no significant difference in bone formation quantity between 100 mg simvastatin and autograft. Histological and immunohistochemistry examination indicated entochondrostosis in association with positive expression of BMP-2 and HIF-1 alpha. Spiral CT-scan and histological examination of calvarial defects of monkeys showed intramembranous ossification after simvastatin implantation. No change was found in the control group.
Conclusions: Topical administration of simvastatin induces entochondrostosis and intramembranous ossification by enhancing expression of BMP-2 and HIF-1 alpha. The effect of simvastatin on bone regeneration is comparable to autograft.
The translational potential of this article: Topical administration of simvastatin can repair bone defect in both long tubular bones and flat bones of rabbits and monkeys as effectively as autograft. Given that it is cheap, safe and already in clinical use, simvastatin might be considered as a bone regeneration inducer with great potential.

Introduction

Bone defect repairmen, as an important yet challenging clinical problem, has long been a topic of tremendous interest in the field of orthopedics. Although significant progress has been made with noticeable success, the issue remains largely unresolved. The repairmen involves a complex bone regeneration process requiring reconstruction of bone structure with adequate function. Conventional treatments including bone graft and various forms of synthetic bone substitutes are flawed either for the significant side effects or for being financially unsound. The latest approach is to utilize tissue-engineering technology whereby osteogenic stem cells and/or bone growth factors are amplified or loaded in extracellular matrices *in vitro* before they are implanted *in vivo* to repair bone defect. The stem cells and the growth factors act to induce bone formation and the matrices serves as a scaffold that gradually degrades along with bone ingrowth. This should endow the new

* Corresponding author. Department of Orthopedics, Peking University 3rd Hospital, Beijing Key Laboratory of Spinal Disease Research, 49 North Garden Rd., Haidian District, Beijing, 100191, PR China.
E-mail addresses: mph595@126.com (L. Dang), schl@bjmu.edu.cn (C. Song).

https://doi.org/10.1016/j.jot.2020.11.009
Received 5 June 2020; Received in revised form 22 November 2020; Accepted 26 November 2020

bone with both adequate structure and function. Nonetheless, the use of stem cells is still in an experimental stage due to the lack of reliable technique in amplifying and guided differentiation [1]. There has been clinical success in the use of bone growth factors in combination with natural polymers scaffold as bone healing materials. But the rising safety concerns and the high cost significantly limits their clinical application [2].

In earlier study of osteoporosis, it was noticed that simvastatin, a drug for lowering serum cholesterol, had an effect to enhance bone formation by increasing expression of the bone morphogenetic protein-2 (BMP-2) gene in bone cells [3]. More recent clinical studies also associate simvastatin with increased bone density and reduced risk of osteoporotic fracture [4,5]. Because it is safe, cheap and clinically available, simvastatin has been drawing increasing attention as a promising new bone regeneration inducer. However, the exact mechanism and effectiveness of simvastatin on bone formation as well as the optimal dose remains unclear. This study is prompted to investigate these issues in search for a better bone regeneration inducer.

Materials and methods

Ethical statement

All experiments performed in this study were approved by the Peking University Third Hospital Animal Experiment Ethics Committee, Permit No. 2009–0006 (2). Animal care complied with the guideline of animal experiments of the Peking University Third Hospital on the care and use of laboratory animals.

Materials

There were two sets of bone defect animal models tested in this study. The first model involved 12 adult male New Zealand rabbits weighed 2.3–2.8 kg. The second model involved three Rhesus monkeys, aged 5–6 years and weighed 7.5–9.5 kg.

General procedures

In the first model, a 22 mm long bone defect was surgically inflicted on the radius of both forearms of each of 12 New Zealand rabbits (Fig. 1A and B) that were randomly divided into four groups. Note that, each time the periosteum of ulna was also removed along with the radius in the making of the defect. In three of the four groups, the radial bone defect was filled with compounds made up of simvastatin (Merck & Co Inc, USA) of three different dosages and poly lactic acid (PLA, molecular weight 4×10^6, Shandong Medical Instrument Research Center, China) scaffold on one side (the implant side) and PLA scaffold alone on the other (the control side). For the implant side, the compound was made under room temperature by mixing simvastatin (50 mg, 100 mg and 200 mg respectively) with 250 ml PLA and 2 ml acetone solution (Sinopharm Chemical Reagent Beijing Co. Ltd, China), which was subsequently freeze-dried and molded to form a 4 mm thick and 24 mm long cylindrical paste (Fig. 1C). It was sterilized by ^{60}Co radiation each time before implantation. For the control side, the compound was made the same way except that no simvastatin was added to the paste. For the remaining group, removed radial bone was minced and re-implanted to the defect as

Table 1
Groups with different interventions in rabbits radial defect model and Rhesus monkey calvarial defect model.

Animal model	Groups	Implant side (left)	Control side (right)
New Zealand rabbit model	SIM50mg	simvastatin 50 mg + PLA 250 mg+2 ml acetone	PLA 250 mg+2 ml acetone
	SIM100mg	simvastatin 100 mg + PLA 250 mg+2 ml acetone	PLA 250 mg+2 ml acetone
	SIM200mg	simvastatin 200 mg + PLA 250 mg+2 ml acetone	PLA 250 mg+2 ml acetone
	Autograft	autogenous bone	void
Rhesus monkey model	SIM50mg	simvastatin 50 mg + thrombin 0.4 ml + fibrin sealant	0.4 ml thrombin+0.4 ml fibrin sealant

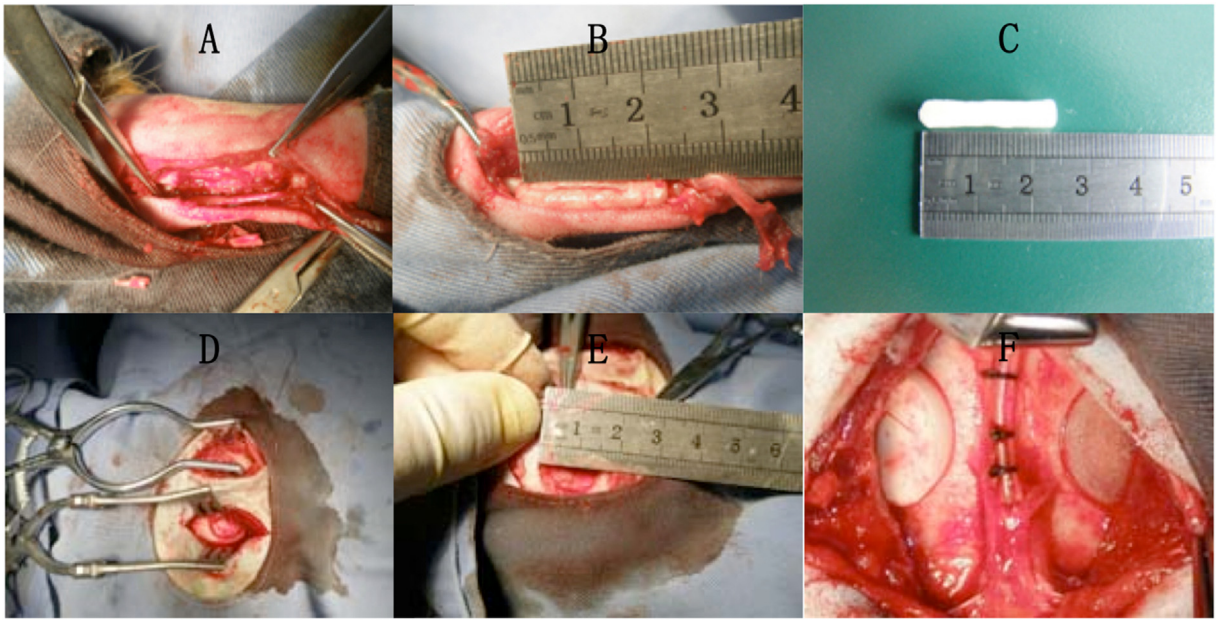

Fig. 1. The New Zealand rabbit radial defect and the Rhesus monkey calvarial defect. A-C. The New Zealand rabbit model. D-F. The Rhesus monkey model. A. Surgically inflicted radial bone defect (without implantation). B. Radial bone defect with simvastatin and PLA implantation. C. A Solid block made of simvastatin and PLA. D. Surgically inflicted bone defects on either side of the sagittal suture (without implantation). E. Each defect was made 15 mm in diameter. F. A 4 mm thick pancake shape paste made of simvastatin/thrombin/FS and thrombin/FS in place of the defect.

autogenous bone graft on the implant side while no intervention was applied on the control side. Detailed information concerning each group was given in Table 1. Repairing progress of the radial bone defects was monitored radiologically at 8 and 16 weeks after surgery and histologically as well as immunohistochemically when all rabbits were eventually sacrificed at the 16th week. In the second model, two full-thickness round defects of 15 mm diameter were made on both sides of the sagittal suture of each of three Rhesus monkeys (Fig. 1D–F). A compound of 50 mg simvastatin, 0.4 ml thrombin and 0.4 ml fibrin sealant (FS) was implanted on the left hand side (the implant side) while the same compound without simvastatin was implanted on the right hand side (the control side). CT scans of the involved calvarias were taken at 2, 4, 6, 12 and 18 weeks post-operation before all subjects were sacrificed for histological examination except for one that was sacrificed 4 weeks into the experiment and subject to histological examination.

Measurements

The rabbit model

Radiological measurements. Bone ingrowth in each radial bone defect was monitored at 8 and 16 weeks post-operation using a digital x-ray machine. For each bone defect, the x-ray pixel values of three identical spots chosen at fixed co-ordinates were measured and scaled using Taria's x-ray scoring method to quantify bone healing in each circumstance [6]. Spiral CT scans (120 kV, 256 mA, thickness 2.0 mm, GE, USA) were taken at 16 weeks post-operation of both forearms of each sacrificed rabbit to reconstruct a 3D image of the intact radial bones using surface shade display (SSD) method. The area of opaque region (representing new bone formation) against the whole area of bone defect was calculated using computer software (GE AW4.2 software) and compared as the ratio of new bone formation in each experimental group. The same method had been described by Nakayama et al. [7]. One rabbit was randomly selected from the implant groups and examined using high-resolution plain film (Hitachi, Japan) and Micro CT scan (Skyscan, Belgium) to inspect structural changes on the surface and in the bone marrow cavity of the bone defects.

Histological inspection. The section of bone defect in each radium was severed to obtain 5 μm-thick slices and processed with hematoxylin-eosin (HE) and toluidine blue staining before being inspected under optical microscopy.

Immunohistochemistry examination. The same slices were immersed with BMP-2 and Hypoxia-inducible factors (HIF)-1alpha antibodies (Santa Cruz Biotechnology Inc, USA and Abcam plc, USA) and dyed to detect expression of BMP-2 and HIF-1alpha using Polymer HRP Detection System for goat primary antibody and Mouse SP Kit (Santa Cruz Biotechnology Inc, USA).

The monkey model

Radiological measurements. Calvarias of two of the three monkeys were scanned using Spiral CT at 2, 4, 6, 12 and 18 weeks post-operation to reconstruct a 3D image of the entire calvarial bone using surface shade display (SSD) method. The remaining monkey was sacrificed at 4 weeks for histological inspection.

Histological inspection. Bone defect sections obtained from the sacrificed monkey were severed to obtain 5 μm-thick slices and processed with hematoxylin-eosin (HE) and toluidine blue staining before being inspected under optical microscopy.

Statistical methods. All statistical tests were carried out using computer software (SPSS 13.0). Results obtained from the implant sides and the control sides were compared within each group using Student t-test and between different groups using One-way analysis and LSD test. Difference was deemed significant when p value was less than 0.05.

Results

The rabbit model

Radiological measurements

X-ray image. Radiographic images demonstrated significant bone healing at 8 weeks post-operation and complete bone union at 16 weeks on the implant sides in all groups. Fig. 2 & Table 2 show callus formation in the defects changed from blurry into continuous and fracture ends changed from blurry to union. By contrast, neither identifiable callus formation nor signs of union at the fracture ends were found on all the control sides for the same period.

X-ray scores. For all experimental groups, the x-ray scores were significantly ($p < 0.05$) greater on the implant sides than the control sides at both 8 and 16 weeks of the experiment. At 8 weeks, the x-ray scores on the implant sides were significantly higher in the SIM200mg and the autograft group than that in the SIM50mg and the SIM100mg group, although there was no significant difference between the former and latter two groups respectively. At 16 weeks, SIM100mg and autograft group were associated with significantly ($p < 0.05$) greater x-ray scores than the rest two groups, without a significant difference between themselves (Table 3).

X-ray pixel values. In all groups, implant sides were associated with significantly greater x-ray pixel values than control sides at both 8 and 16 weeks post-operation. There was no significant difference among implant groups and control groups respectively (Table 3).

Spiral CT scans. Bone union or significant reduction in bone defect was seen on the implant sides whereas non-union and insignificant bone ingrowth was seen on the control sides of all SIM groups and the autograft group (Fig. 3A–D). The ratio of new bone formation was significantly higher on the implant side than the control side in all groups with the SIM 100 mg and autograft group being associated with significantly higher rates than the rest (Fig. 4).

High-resolution plain film and micro CT scans. Both forearms of one rabbit in the SIM 100 mg group (Fig. 3B) were scanned. The images of the implant side showed the defect was replaced by continuous new bone formation with union at both fracture ends, complete cortical bone formation on the outside and rechanellization of bone marrow cavity on the inside (Fig. 3E&F). On the control side, neither continuous bone formation nor rechanellization of bone marrow was seen (Fig. G&H).

Histological inspection

HE staining. Radial bone defects were replaced by new bone formation with complete cortical bone and closed medullary cavities on the implant sides in all groups whereas no bone formation but hyperplasia was found on the control sides (Fig. 5A).

Toluidine blue staining. Visual inspection under microscopy showed transformation of mesenchymal cells to chondrocytes and eventually to bone tissues in most area of the defect on the implant side (SIM 100 mg). There were a few residual chondrocytes in sight (Fig. 5B). On the control side, large portion of deep blue staining area indicates lack of transformation from chondrocytes to bone tissues.

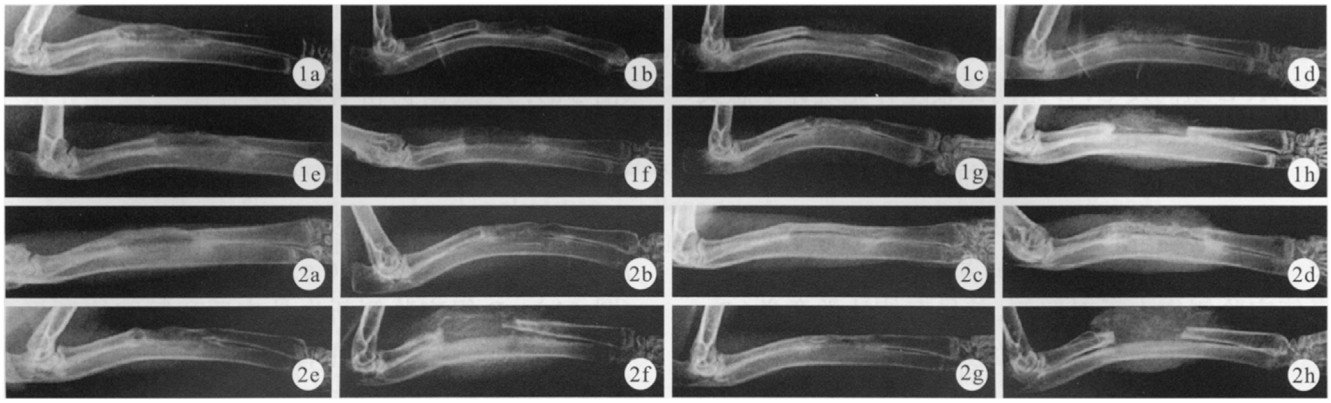

Fig. 2. Radiographs of radial defects at 8 and 16 weeks after simvastatin implantation. 1a-1h. Radiographs at 8 weeks. 1a. SIM50mg implant side. 1 b. SIM50mg control side. 1c. SIM100mg implant side. 1 d. SIM100mg control side. 1e. SIM200mg implant side. 1f. SIM200mg control side. 1 g. Autograft implant side. 1 h. Autograft control side. 2a-2h. Radiographs at 16 weeks. 2a. SIM50mg implant side. 2 b. SIM50mg control side. 2c. SIM100mg implant side. 2 d. SIM100mg control side. 2e. SIM200mg implant side. 2f. SIM200mg control side. 2 g. Autograft implant side. 2 h. Autograft control side.

Table 2
Radiographic images of rabbit radial defect model.

Groups	8 weeks				16 weeks			
	callus formation		fracture ends		callus formation		fracture ends	
	IS*	CS*	IS*	CS*	IS*	CS*	IS*	CS*
SIM50mg	hazy	none or few	blurry	clear	continuous	none or few	union	Sclerotic
SIM100mg	even	none or few	blurry	clear	continuous	none or few	union	Sclerotic
SIM200mg	continuous	none or few	continuous	clear	continuous	none or few	union	sclerotic
Autograft	abundant	none or few	blurry	clear	continuous	none or few	union	sclerotic

Table 3
Comparison of x-ray scores and pixel values measured from the bone defects at 8 and 16 weeks post-op among all experimental groups.

Items	Groups	8 weeks post-op		16weeks post-op	
		IS*	CS*	IS*	CS*
x-ray scores	SIM50mg	7.17 ± 0.75*△▲	5.67 ± 0.82	11.83 ± 1.47*#▲	8.67 ± 1.03
	SIM100mg	8.00 ± 0.63*△▲	6.33 ± 1.03	17.00 ± 0.89*△	8.50 ± 1.05
	SIM200mg	9.67 ± 1.03*#	4.83 ± 0.98	9.67 ± 1.21*#▲	5.67 ± 1.37
	autograft	9.50 ± 1.05*#	5.17 ± 1.17	18.17 ± 1.47*△	5.00 ± 0.89
Pixel values	SIM50mg	1.42 ± 0.04*	0.83 ± 0.04	3.44 ± 0.09*	2.41 ± 0.03
	SIM100mg	1.82 ± 0.12*	1.37 ± 0.06	3.68 ± 0.05*	2.59 ± 0.08
	SIM200mg	1.47 ± 0.93*	1.09 ± 0.05	3.49 ± 0.02*	2.48 ± 0.08
	Autograft	1.43 ± 0.13*	1.10 ± 0.11	3.45 ± 0.03*	2.42 ± 0.07

* IS=Implant Side; CS=Control Side *$p < 0.05$ as compared with CS; #$p < 0.05$ as compared with SIM100mg group; △$p < 0.05$as compared with SIM200mg group; ▲$p < 0.05$ as compared with autograft group

Immunohistochemistry examination. Expression of BMP-2 (Fig. 6A) and HIF-1 alpha (Fig. B) was positive under optical microscope on the implant side at 16 weeks after implantation.

The monkey model

Spiral CT scans. Traces of high-density bone formation started to emerge in calvarial defects of all three monkeys since 6 weeks into the study and gradually developed on the implant side until the end of the experiment (18 weeks) when the defect was significantly reduced. By contrast, no change was visible on the control side all through the experiment (Fig. 7).

HE staining. HE staining of the calvarial bone defect at 4 weeks after simvastatin implantation showed islands of newly formed woven bone spreading in a matrix of mesenchymal cells in absence of chondrocytes on the implant side (Fig. 8A and B). On the control side, however, there was no bone formation but inflammatory and fibrous tissue (Fig. 8C and D).

Discussion

This study is designed to explore effects of simvastatin on different mechanisms of bone development. Rabbit radial defect and monkey calvarial defect model were used in this study to investigate the effect of simvastatin on both entochondrostosis of long tubular bones and intramembranous ossification of flat bones respectively. Radial defect of rabbits is considered the standard model in study of bone formation where a 20 mm long bone defect is deemed the upper limit for self-repairmen [8]. We used 22 mm long bone defects in excess of the maximal limit for self-repairmen. The periosteum of the ulna was also removed to eliminate interference from bone formation originated from the ulna. Design of the self-controlled study also helps to minimize the potential interference from the ulna. Monkeys are considered the most genetically close to human.

This study compared the result of the experiment and the control group on two symmetrical sides of the same subject, which eliminated influence of individual difference. In the rabbit radial model, X-ray images showed union of bone defect in all simvastatin-implanted groups in comparison with absence of bone formation in all control groups. Micro CT scans showed newly formed bone with complete cortex and rechanellization of bone marrow cavity. These suggested that simvastatin acted to induce natural bone healing while being released and biodegraded in the bone defect. X-ray scores, X-ray pixel values and spiral CT scans measurements are widely accepted standard methods for quantitative assessment of osteogenesis, which confirmed the visual

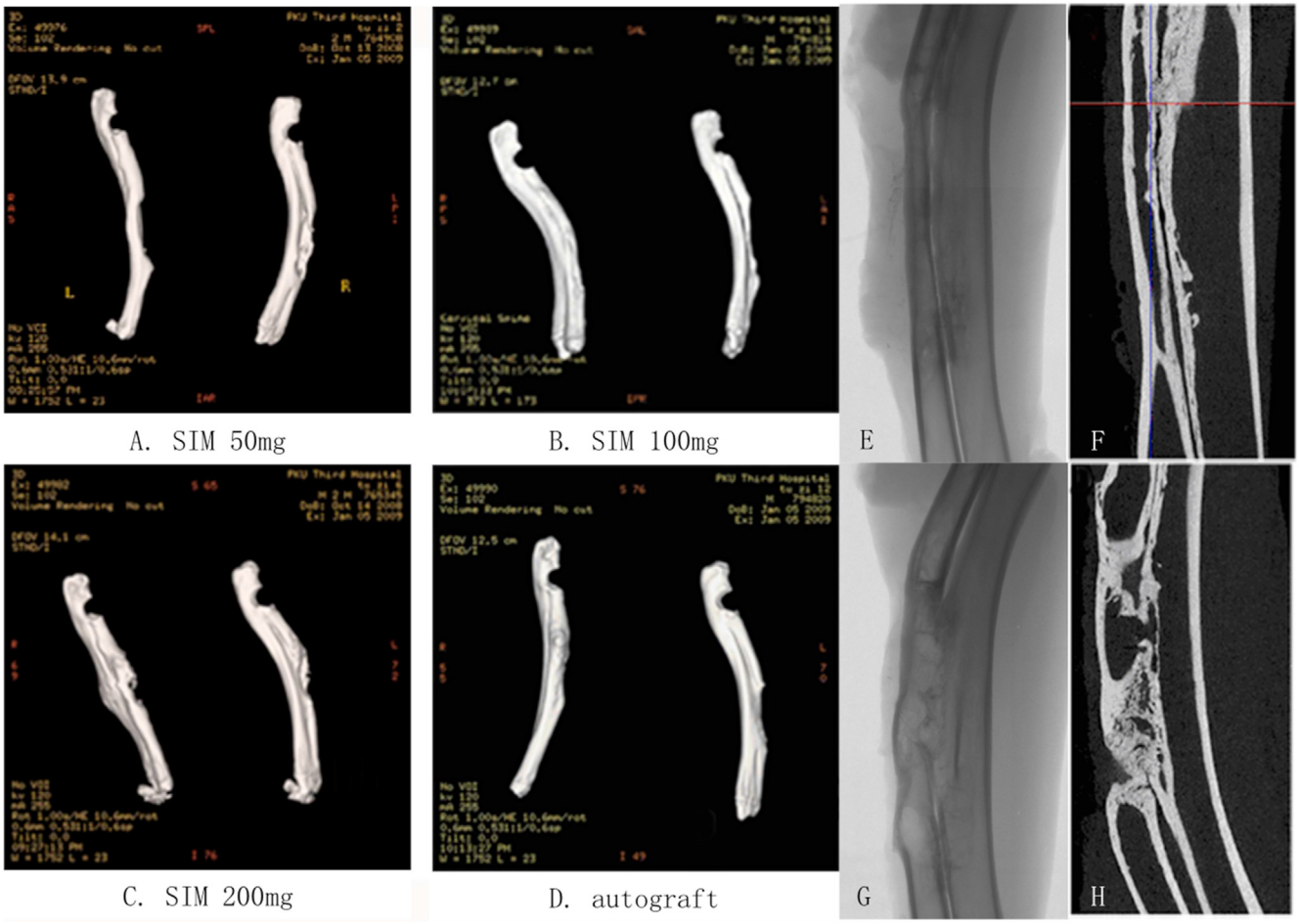

Fig. 3. Spiral CT scans of radial defects on the implant and the control sides in all experimental groups at 16 weeks after simvastatin implantation. (A-D). Spiral CT scans (Right: Implant side; Left: Control side). E&F. High-resolution plain film (E) and Micro CT scan (F) of the defect on the implant side in the SIM100mg group. G&H. High-resolution plain film (G) and Micro CT scan (H) of the defect on the control side in the SIM100mg group.

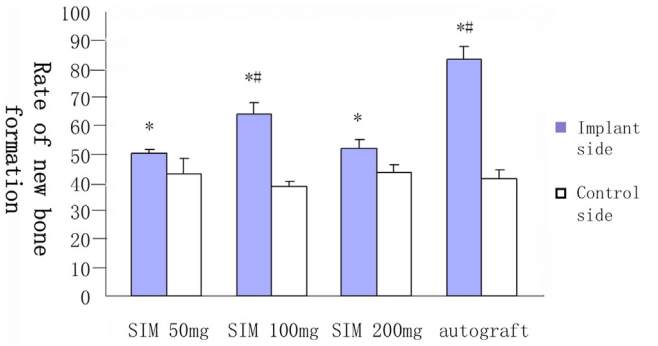

Fig. 4. Rates of new bone formation in radial defects measured from spiral CT scans at 16 weeks after simvastatin implantation. Note that there were 6 radial bone defects from 3 different rabbits tested in each group in the plot. *significant difference between Implant and Control side ($p < 0.05$); #significant difference between SIM 100 mg, autograft group and SIM 50 mg, SIM 200 mg group ($p < 0.05$). 120 kV 256 mA thin-bed layer thickness 0.625 mm.

finding by showing a significantly higher density and ratio of new bone formation on the implant sides than that on the control sides [9]. These quantitative radiological findings were further verified histologically by HE and Toluidine blue staining. Toluidine blue is known to have an affinity for proteoglycans in the chondrocytes [10]. Changes in the staining demonstrated transformation of mesenchymal cells to chondrocytes and to bone tissues. Residual chondrocytes were also evidences of entochondrostosis.

The function of simvastatin to enhance bone formation and reduce bone loss was initially demonstrated after gastric administration and subcutaneous tissue injection in rats [11,12]. Seto et al. and Lee et al. later reported significant repairmen of bone defects in the alveolar bone and the mandibles of rats after topical application of simvastatin [13,14]. More recent studies succeed to test the effect of local administration of simvastatin on bone regeneration using bigger animal models. Chalisserry et al. created 24 5 × 8 mm bone defects on the lateral aspect of the femoral condyle of 12 adult New Zealand white rabbits to compare the result of bone formation induced by Nano-Hydroxyapatite (nHA) particles alone and nHA with simvastatin. The condyles were retrieved after 8 weeks and analyzed using micro CT and histology. Their results showed significantly higher bone mineral density and bone volume in the simvastatin loaded nHA group compared with the nHA alone group [15]. Zhang et al. reported the same result when compared the effect of simvastatin loaded Polylactic Acid-Polyglycolic Acid Copolymer (PLGA-CPC) with that of PLGA-CPC alone on rabbit femoral condyle defects [16]. These are concordant with our results even though we used maximum size radial bone defects that represent the most extreme model of entochondrostosis in long tubular bones. Positive effect of simvastatin on bone formation in calvarias has been reported using different carriers in rats and rabbits [17–19]. But there is a lack of similar study using nonhuman primates. Yasuhiko et al. implanted a basic fibroblast growth factor (bFGF) loaded biodegradable hydrogel to skull defects (6 mm in diameter) in a monkey [20]. The defects were replaced by new bone formation in 21 weeks after implantation. We used monkeys calvarial

Fig. 5. HE and Toluidine blue staining images of radial defects under optical microscope at 16 weeks after simvastatin implantation. A. HE staining (× 10) of the implant side (left column) and the control side (right column). U: ulna; R: radius. B. Toluidine blue staining (× 100) of the implant side (left) and the control side (right).

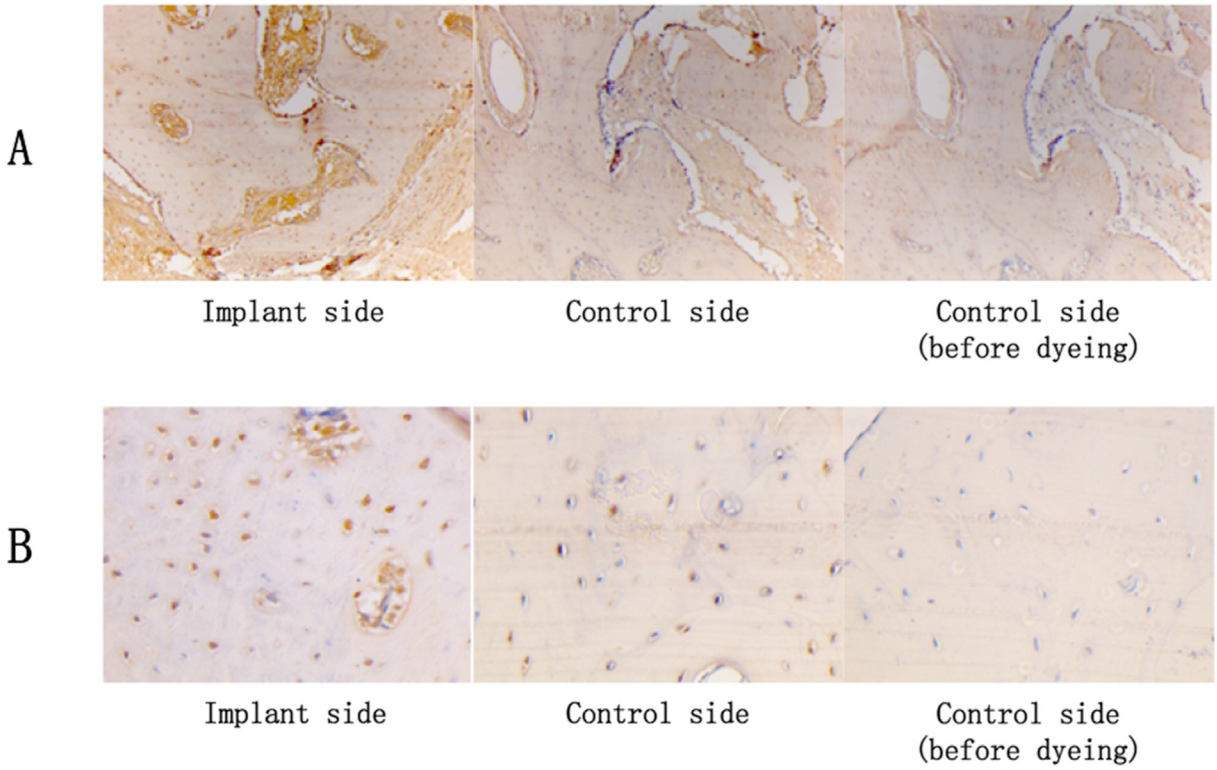

Fig. 6. Expression of BMP-2 in cytoplasm and HIF-1 alpha in cell nucleus under optical microscope at 16 weeks after simvastatin implantation. A. Expression of BMP-2 in cytoplasm (× 100). B. Expression of HIF-1 alpha in cell nucleus (× 400).

model because monkeys were genetically closer to human than any other animals and the calvarial bone was the site to choose for investigation of intramembranous ossification in flat bones. In our study, Spiral CT scans showed significantly reduced bone defects at 18 weeks after implantation on the implant side and no change on the control side. This was verified by HE staining, which showed widespread newly formed woven bone in a matrix of mesenchymal cells on the implant side. The absence of chondrocytes indicates origin of bone formation from transformation of mesenchymal cells, i.e. intramembranous ossification.

Our results of immunohistochemistry examination indicated positive expression of BMP-2 and HIF-1 alpha after simvastatin implantation. HIFs are oxygen-dependent transcriptional activators that play crucial roles in angiogenesis, erythropoiesis, energy metabolism, and cell fate decisions. HIFs and their target gene, vascular endothelial growth factor (VEGF), are believed to promote bone regeneration by stimulating new blood vessels formation in the bone [21–23]. BMP-2 is a known growth factor that induces bone regeneration. Numerous studies suggest that simvastatin can promote osteoblast viability and differentiation by enhancing expression of BMP-2 [3,18,24]. The potential mechanism is that simvastatin inhibits the secretion of mevalonic acid, which per se is an inhibitor of BMP-2, by blocking the action of the HMG-CoA reductase [25]. Moreover, inhibition of mevalonic acid also impedes activation of osteoclast [26].

Simvastatin presents a reduced risk in comparison with growth factors or gene therapy, but undesired high local congregation may still pose a risk of inflammatory response [27]. Therefore, it requires a carrier that can slow the release process allowing simvastatin to function for an extended period while limiting the inflammatory process. PLA is known as a biocompatible and biodegradable polymer with a three dimensional porous structure that facilitates bone ingrowth [28]. Previous studies of PLA and simvastatin compound proved that release of simvastatin could be controlled by the slow degradation of PLA due to the strong chemical interaction between the two [29–31]. Moreover, mechanical property of the scaffold was not influenced during the release process.

Although simvastatin has been investigated as a bone regeneration inducer in multiple forms of administration, there has no general consent on the optimal dose to date. The dosage used in this study was determined based on relevant reviews in the literature [32]. In this study, x-ray scores of the SIM100mg and autograft were significant higher than the rest groups whereas no difference was found between each other. The same result was confirmed by spiral CT scans in calculation of the ratio of new bone formation. Both quantitatively verified the effect of simvastatin. Our results of significant association between higher concentration of simvastatin and higher X-ray scores can be explained as previous studies indicated a positive correlation between the dose of simvastatin and expression of BMP-2 [3,33]. However, the finding that 100 mg simvastatin group had significantly higher X-ray scores and new bone formation rate than 200 mg simvastatin group at 16 weeks after implantation seemed to indicate an optimal dose for topical administration. In fact, we found in preparation of SIM200mg implant that its porosity was significantly lower than that of SIM50mg and SIM100mg implant. Low porosity could impede bone growth by limiting ingrowth of blood vessels and mesenchymal cells. Other authors suggested that time also had significantly influences on the effect of simvastatin [32].

The weakness of this study is that it is an animal experiment. But it is the first time that simvastatin is tested in non-human primate. In addition, the limited number of samples involved in this study limits the statistical power of the result and makes it erring on the side of caution. The encouraging results of ours favor further clinical tests for topical administration of simvastatin as a bone regeneration inducer.

Conclusions

Topical administration of simvastatin can promote bone regeneration in both forms of entochondrostosis and intramembranous ossification with a capacity comparable to autograft. It also acts in different species of mammals, including non-human primates. Its effect on entochondrostosis is associated with increased expression of BMP-2 and HIF-1

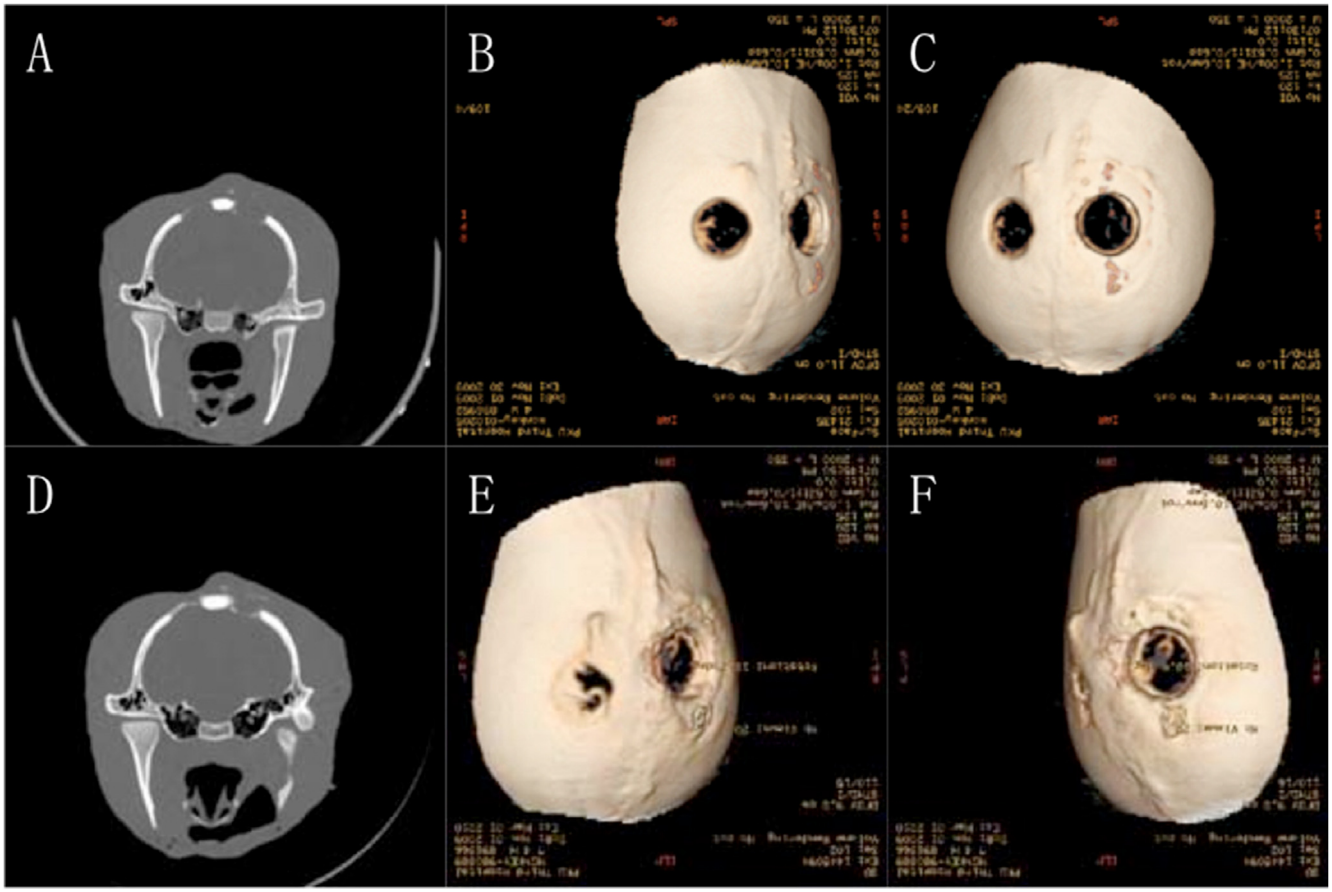

Fig. 7. Spiral CT scans of calvarial defects on the implant and the control sides at 6 and 18 weeks after simvastatin implantation. A-C. 6 weeks post-op. A. Coronal plane showing the implant side (left) and the control side (right). B&C. 3D-reconstruction images showing the implant side (left) and the control side (right). D-F. 18 weeks post-op. D. Coronal plane showing the implant side (left) and the control side (right). E&F. 3D-reconstruction image showing the implant side (left) and the control side (right).

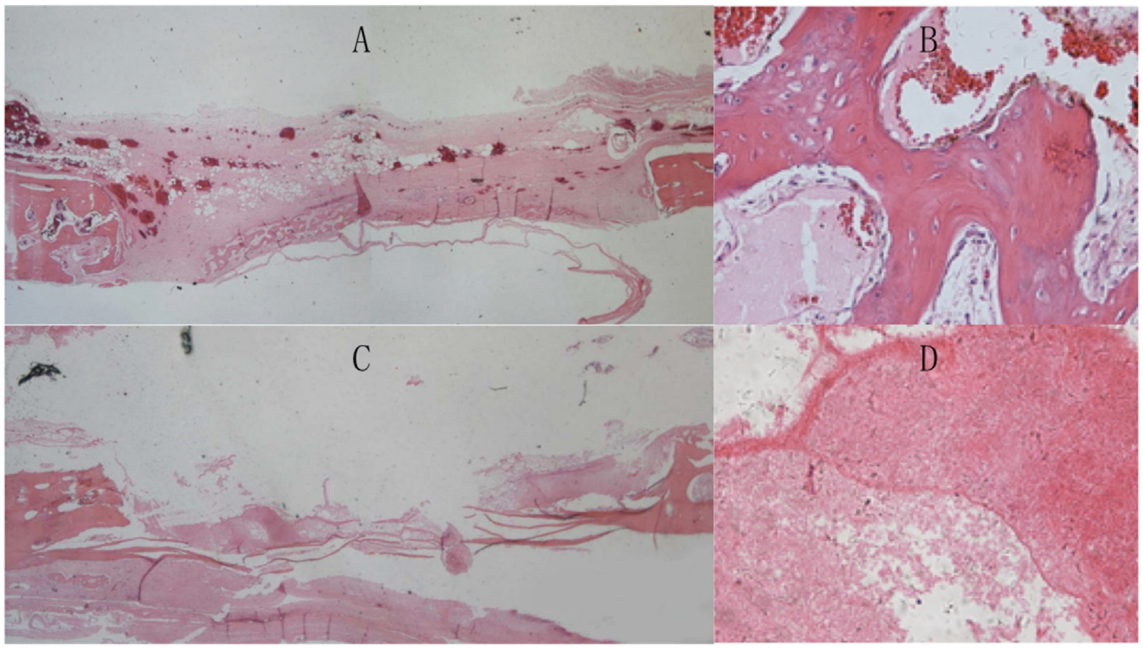

Fig. 8. HE staining images of calvarial defects under optical microscope at 4 weeks after simvastatin implantation. A-B. The implant side. A. Woven bone formation can be seen spreading across the defect (× 10). B. Magnified image showing woven bone formation (× 200). C-D. The control side. No bone formation but inflammatory tissue can be seen (× 10, × 200).

alpha. Therefore, simvastatin is a promising candidate for the best bone regeneration inducer.

Funding

This work was supported by grants from the National Natural Science Foundation of China (Grant Number 81672133, 81874010) and the National High Technology Research and Development Program of China (863 Program, grant number 2015AA020304).

Declaration of competing interest

The authors have no conflicts of interest relevant to this article.

Appendix A. Supplementary data

Supplementary data to this article can be found online at https://doi.org/10.1016/j.jot.2020.11.009.

References

[1] Walmsley GG, Ransom RC, Zielins ER, Leavitt T, Flacco JS, Hu MS, et al. Stem cells in bone regeneration. Stem cell reviews and reports 2016;12(5):524–9 [eng].
[2] Dumic-Cule I, Peric M, Kucko L, Grgurevic L, Pecina M, Vukicevic S. Bone morphogenetic proteins in fracture repair. Int Orthop 2018;42(11):2619–26 [eng].
[3] Mundy G, Garrett R, Harris S, Chan J, Chen D, Rossini G, et al. Stimulation of bone formation in vitro and in rodents by statins. Science 1999;286(5446):1946–9.
[4] An T, Hao J, Sun S, Li R, Yang M, Cheng G, et al. Efficacy of statins for osteoporosis: a systematic review and meta-analysis. Osteoporos Int : a J. Establish. Res. Cooper. Betn. Eur. Found. Osteopor. Natl. Osteopor. Found. USA 2017;28(1):47–57 [eng].
[5] Chiadika SM, Shobayo FO, Naqvi SH, Saraykar SS, Ambrose CG, Rianon NJ. Lower femoral neck bone mineral density (BMD) in elderly women not on statins. Women Health 2019;59(8):845–53 [eng].
[6] Taira H, Moreno J, Ripalda P, Forriol F. Radiological and histological analysis of cortical allografts: an experimental study in sheep femora. Arch Orthop Trauma Surg 2004;124(5):320–5.
[7] Nakayama Y, Li Q, Katsuragawa S, Ikeda R, Hiai Y, Awai K, et al. Automated hepatic volumetry for living related liver transplantation at multisection CT. Radiology 2006;240(3):743–8 [eng].
[8] Saito A, Suzuki Y, Kitamura M, Ogata S, Yoshihara Y, Masuda S, et al. Repair of 20-mm long rabbit radial bone defects using BMP-derived peptide combined with an alpha-tricalcium phosphate scaffold. J Biomed Mater Res 2006;77(4):700–6 [eng].
[9] Hazra S, Song HR, Biswal S, Lee SH, Lee SH, Jang KM, et al. Quantitative assessment of mineralization in distraction osteogenesis. Skeletal Radiol 2008;37(9):843–7.
[10] Vidal BC, Mello MLS. Toluidine blue staining for cell and tissue biology applications. Acta Histochem 2019;121(2):101–12 [eng].
[11] Serin-Kilicoglu S, Erdemli E. New addition to the statin's effect. J Trauma 2007;63(1):187–91.
[12] Oxlund H, Dalstra M, Andreassen TT. Statin given perorally to adult rats increases cancellous bone mass and compressive strength. Calcif Tissue Int 2001;69(5):299–304.
[13] Seto H, Ohba H, Tokunaga K, Hama H, Horibe M, Nagata T. Topical administration of simvastatin recovers alveolar bone loss in rats. J Periodontal Res 2008;43(3):261–7.
[14] Lee Y, Schmid MJ, Marx DB, Beatty MW, Cullen DM, Collins ME, et al. The effect of local simvastatin delivery strategies on mandibular bone formation in vivo. Biomaterials 2008;29(12):1940–9.
[15] Chalisserry EP, Nam SY, Anil S. Simvastatin loaded Nano hydroxyapatite in bone regeneration: a study in the rabbit femoral condyle. Curr Drug Deliv 2019;16(6):530–7 [eng].
[16] Zhang HX, Xiao GY, Wang X, Dong ZG, Ma ZY, Li L, et al. Biocompatibility and osteogenesis of calcium phosphate composite scaffolds containing simvastatin-loaded PLGA microspheres for bone tissue engineering. J Biomed Mater Res 2015;103(10):3250–8 [eng].
[17] Venkatesan N, Liyanage ADT, Castro-Nunez J, Asafo-Adjei T, Cunningham LL, Dziubla TD, et al. Biodegradable polymerized simvastatin stimulates bone formation. Acta Biomater 2019;93:192–9 [eng].
[18] Zhang J, Wang H, Shi J, Wang Y, Lai K, Yang X, et al. Combination of simvastatin, calcium silicate/gypsum, and gelatin and bone regeneration in rabbit calvarial defects. Sci Rep 2016;6:23422 [eng].
[19] Wang CZ, Wang YH, Lin CW, Lee TC, Fu YC, Ho ML, et al. Combination of a bioceramic scaffold and simvastatin nanoparticles as a synthetic alternative to autologous bone grafting. Int J Mol Sci 2018;19(12) [eng].
[20] Tabata Y, Yamada K, Hong L, Miyamoto S, Hashimoto N, Ikada Y. Skull bone regeneration in primates in response to basic fibroblast growth factor. J Neurosurg 1999;91(5):851–6 [eng].
[21] Fan L, Li J, Yu Z, Dang X, Wang K. The hypoxia-inducible factor pathway, prolyl hydroxylase domain protein inhibitors, and their roles in bone repair and regeneration. BioMed Res Int 2014;2014:239356 [eng].
[22] Weimin P, Zheng C, Shuaijun J, Dan L, Jianchang Y, Yue H. Synergistic enhancement of bone regeneration by LMP-1 and HIF-1alpha delivered by adipose derived stem cells. Biotechnol Lett 2016;38(3):377–84 [eng].
[23] Jiang X, Zhang Y, Fan X, Deng X, Zhu Y, Li F. The effects of hypoxia-inducible factor (HIF)-1alpha protein on bone regeneration during distraction osteogenesis: an animal study. Int J Oral Maxillofac Surg 2016;45(2):267–72 [eng].
[24] Chen PY, Sun JS, Tsuang YH, Chen MH, Weng PW, Lin FH. Simvastatin promotes osteoblast viability and differentiation via Ras/Smad/Erk/BMP-2 signaling pathway. Nutr Res (NY) 2010;30(3):191–9 [eng].
[25] Montagnani A, Gonnelli S, Cepollaro C, Pacini S, Campagna MS, Franci MB, et al. Effect of simvastatin treatment on bone mineral density and bone turnover in hypercholesterolemic postmenopausal women: a 1-year longitudinal study. Bone 2003;32(4):427–33 [eng].
[26] Luckman SP, Hughes DE, Coxon FP, Graham R, Russell G, Rogers MJ. Nitrogen-containing bisphosphonates inhibit the mevalonate pathway and prevent post-translational prenylation of GTP-binding proteins, including Ras. J Bone Miner Res : Off. J. Am. Soc. Bone and Miner. Res. 1998;13(4):581–9 [eng].
[27] Encarnacao IC, Xavier CC, Bobinski F, dos Santos AR, Correa M, de Freitas SF, et al. Analysis of bone repair and inflammatory process caused by simvastatin combined with PLGA+HA+betaTCP scaffold. Implant Dent 2016;25(1):140–8 [eng].
[28] Kotsar A, Nieminen R, Isotalo T, Mikkonen J, Uurto I, Kellomaki M, et al. Biocompatibility of new drug-eluting biodegradable urethral stent materials. Urology 2010;75(1):229–34 [eng].
[29] Hu Z, Liu Y, Yuan W, Wu F, Su J, Jin T. Effect of bases with different solubility on the release behavior of risperidone loaded PLGA microspheres. Colloids Surf B Biointerfaces 2011;86(1):206–11 [eng].
[30] Montazerolghaem M, Rasmusson A, Melhus H, Engqvist H, Karlsson Ott M. Simvastatin-doped pre-mixed calcium phosphate cement inhibits osteoclast differentiation and resorption. J Mater Sci Mater Med 2016;27(5):83 [eng].
[31] Encarnacao IC, Sordi MB, Aragones A, Muller CMO, Moreira AC, Fernandes CP, et al. Release of simvastatin from scaffolds of poly(lactic-co-glycolic) acid and biphasic ceramic designed for bone tissue regeneration. J Biomed Mater Res B Appl Biomater 2019;107(6):2152–64 [eng].
[32] Sendyk DI, Deboni MC, Pannuti CM, Naclerio-Homem MG, Wennerberg A. The influence of statins on osseointegration: a systematic review of animal model studies. J Oral Rehabil 2016;43(11):873–82 [eng].
[33] Mankani MH, Kuznetsov SA, Shannon B, Nalla RK, Ritchie RO, Qin Y, et al. Canine cranial reconstruction using autologous bone marrow stromal cells. Am J Pathol 2006;168(2):542–50 [eng].